



Article (refereed) - postprint

Ragab, Ragab. 2015. **Integrated management tool for water, crop, soil and N-fertilizers: the Saltmed model**. *Irrigation and Drainage*, 64 (1). 1-12.
[10.1002/ird.1907](https://doi.org/10.1002/ird.1907)

Copyright © 2015 John Wiley & Sons Ltd

This version available <http://nora.nerc.ac.uk/510959/>

NERC has developed NORA to enable users to access research outputs wholly or partially funded by NERC. Copyright and other rights for material on this site are retained by the rights owners. Users should read the terms and conditions of use of this material at <http://nora.nerc.ac.uk/policies.html#access>

This document is the author's final manuscript version of the journal article, incorporating any revisions agreed during the peer review process. Some differences between this and the publisher's version remain. You are advised to consult the publisher's version if you wish to cite from this article.

The definitive version is available at <http://onlinelibrary.wiley.com>

Contact CEH NORA team at
noraceh@ceh.ac.uk

Integrated Management Tool for Water, Crop, Soil and N-Fertilizers: The SALTMED Model

Abstract

Good management will be required to double food production by 2050. Testing management strategies is commonly carried out in the field. Such trials are costly and require quite a long time to produce consistent and reliable results. An alternative option to field trials would be the use of tested models. Models can run with “what-if“scenarios depicting different field management. They are less costly and faster alternative to field trials.

SALTMED 2013 model is designed for general applications that include various irrigation systems, water of different qualities, variety of crops and trees and different soil types. SALTMED model has been tested using field experiment data of Portugal, Italy, Denmark, Morocco, Egypt, Syria, Brazil and Iran. The SALTMED model successfully simulated soil moisture, salinity, nitrogen content, grain yield and total dry matter.

The model provides academics, professionals and extension services with a management tool for crops, soil, water and nitrogen fertilizers. This paper describes the processes, the equations of the model and summarises the different applications and results obtained. This paper will be followed by a number of detailed papers dedicated to the model application and the impact of different field management strategies on food production.

Key Words: SALTMED model, Salinity, Soil moisture, Yield, Dry Matter, Nitrogen fertilizers, Agricultural Water Management

1. Introduction

If the prediction that the world population would increase by a third by 2050 were correct, food production would need to be doubled to feed the population. Do we have enough natural resources, i.e. water, land and nutrients, to produce enough food to feed 9 billion by 2050? Agriculture would have to use the natural resources more efficiently, which means produce more crop per drop and more crop per unit area. Testing a variety of management strategies to maximize food production with minimal input is commonly done by conducting field experiments. Such trials are costly and require a long time to produce consistent and reliable results. An alternative approach would be to use models, as these can be run with “what if” scenarios depicting different field management strategies without the need to run a large number of field trials. Running reliable tested models is less costly than doing field experiments and results could be produced in minutes or hours.

The main resources limiting food production are fertile land, mined fertilizers (phosphorus and potassium) and water. At present, agricultural water use accounts for about 70% of the world’s fresh water use and this percentage is bound to increase if the growing food demand is to be met. In some parts of the world this has already lead to significant overexploitation of conventional water resources and the use of alternative water resources. Even in humid regions, drought events have increased in frequency and the rainfed agriculture regularly has to be supported by supplemental irrigation. The use of non-conventional water resources (e.g. reused agricultural drainage water, treated waste water, brackish groundwater, seawater) requires a great deal of care in order to avoid harming the environment or causing soil degradation (Hamdy *et al.*, 2003; Malash *et al.*, 2005, 2008 and 2011; Huibers *et al.*, 2005, Plauborg *et al.*, 2010, Choukr-Allah , 2012, Pulvanto *et al.*, 2013). In addition deficit irrigation, where the plant is subjected to mild stress in the later, less sensitive, growth stages is being adopted (Hirich *et al.*, 2012, 2013; Silva *et al.*, 2012). Water previously classified as too saline for conventional agriculture is now being used in irrigation (Rhoades *et al.*, 1992). Pulvanto *et al.* (2013) showed that, under an appropriate management system, saline water can be used to irrigate quinoa and amaranth. As salt and water movements are intimately tied, salinity management is dependent on irrigation water management. With the increased use of poor quality water for irrigation an integrated approach is required to minimise drainage disposal problems and optimise the combined use of multiple water sources. As the effect of the use of poor quality water on soil salinity and crop yield only becomes clear after a prolonged period of time, short term experiments are not suitable for studying its long term impact and the use of models can be attractive. Models can also help in irrigation scheduling, estimation of crop water requirements, prediction of soil moisture deficit, soil salinity, soil nutrient status, dry matter production and crop yield.

The SALTMED model (Ragab, 2002, 2005, 2010) was developed to predict final yield, dry matter, soil moisture and soil salinity profiles, plant water and nitrogen uptake, soil nitrogen transformation and content, drainage flow and evapotranspiration. The model can be used for rainfed and irrigated agriculture, as well as for different irrigation systems and irrigation strategies, it accounts for the presence of drainage systems and shallow groundwater. Moreover, the model can handle different crops, soil types and N-fertilizer applications. SALTMED is a physically based model, user friendly (Windows™ environment) and, together with the user guide and related documents, is freely downloadable from the International Commission on Irrigation and Drainage, ICID web site at:

http://www.icid.org/res_tools.html

2. SALTMED model's main processes

The first version of SALTMED (Ragab, 2002) has been updated to include more processes, which will here be described briefly.

2.1. Evapotranspiration

Evapotranspiration has been calculated using the Penman-Monteith equation according to the modified version of FAO (Allen *et al.*, 1998):

$$ET_o = \frac{0.408\Delta(R_n - G) + \gamma \frac{900}{T + 273} U_2 (e_s - e_a)}{\Delta + \gamma(1 + 0.34U_2)} \quad (1a)$$

ET_o is the reference evapotranspiration, (mm day^{-1}), R_n is the net radiation, ($\text{MJ m}^{-2} \text{day}^{-1}$), G is the soil heat flux density ($\text{MJ m}^{-2} \text{day}^{-1}$), T is the mean daily air temperature at 2m height ($^{\circ}\text{C}$), Δ is the slope of the saturated vapour pressure curve ($\text{kPa } ^{\circ}\text{C}^{-1}$), γ is the psychrometric constant, $66 \text{ Pa } ^{\circ}\text{C}^{-1}$, e_s is the saturated vapour pressure at air temperature (kPa), e_a is the prevailing vapour pressure (kPa), and U_2 is the wind speed at 2m height (m s^{-1}).

The ET_o represents short well-watered grass. In this equation, a hypothetical reference crop (height of 0.12m, a fixed surface resistance of 70 s m^{-1} and an albedo of 0.23) was considered.

The SALTMED model also has the option to apply the original Penman-Monteith equation (Monteith 1965) which requires canopy conductance values. The equation takes the form:

$$\lambda E_p = \frac{\Delta R_n + \rho C_p \frac{(e_s - e)}{r_a}}{\Delta + \gamma \frac{(1 + r_s)}{r_a}} \quad (1b)$$

Here, r_a and r_s are aerodynamic and the bulk surface resistances, respectively ($s\ m^{-1}$).

The r_s can be measured, estimated from environmental and meteorological parameters (Jarvis, 1967; Körner, 1994 & 1995) or calculated from the leaf water potential and Abscisic Acid, ABA (Tardieu *et al.*, 1993).

SALTMED model can also use Class A pan evaporation data to calculate ET_o . The model can also calculate net radiation from solar radiation.

The crop evapotranspiration ET_c can be calculated as:

$$ET_c = ET_o (K_{cb} + K_e) \quad (2)$$

K_{cb} is the crop transpiration coefficient and K_e is the bare soil evaporation coefficient. The values of K_{cb} and K_c , (the crop coefficient) for each growth stage, and the length of each growth stage for large number of crops are available in the model's database.

2.2. Plant Water Uptake in Presence of Saline Water

Actual Water Uptake Rate

SALTMED uses the formula suggested by Cardon and Letey (1992), which determines the water uptake S ($mm\ day^{-1}$) as:

$$S(z, t) = \left[\frac{S_{max}(t)}{1 + \left(\frac{a(t)h + \pi}{\pi_{50}(t)} \right)^3} \right] \lambda(z, t) \quad (3)$$

where

$$\lambda(z) = 5/3L \quad \text{for} \quad z \leq 0.2L \quad (4)$$

$$= 25/12L * (1 - z/L) \quad \text{for} \quad 0.2L < z \leq L \quad (4a)$$

$$= 0.0 \quad \text{for} \quad z > L \quad (4b)$$

$S_{max}(t)$ is the maximum potential root water uptake at the time t ; z is the vertical depth, $\lambda(z, t)$ is the depth-and time-dependent fraction of total root mass, L is the maximum rooting depth, π is the osmotic pressure head; h is the matric pressure head, $\pi_{50}(t)$ is the time-dependent value of the osmotic pressure at which $S_{max}(t)$ is reduced by 50%, and $a(t)$ is a weighing coefficient that accounts for the differential response of a crop to matric and solute pressure. The coefficient $a(t)$ equals $\pi_{50}(t)/h_{50}(t)$ where $h_{50}(t)$ is the matric pressure at which $S_{max}(t)$ is reduced by 50%.

The potential water uptake $S_{\max}(t)$ is calculated as:

$$S_{\max}(t) = ET_o(t) * K_{cb}(t) \quad (5)$$

The values of h_{50} and π_{50} are obtainable from measurements or from literature (FAO-48 (Rhoades *et al.*, 1992).

Rooting Depth

The rooting depth was assumed to follow the same path of the crop coefficient K_c and therefore was described by the following equation:

$$\text{Root depth}(t) = [\text{Root depth}_{\min} + (\text{Root depth}_{\max} - \text{Root depth}_{\min})] * K_c(t) \quad (6)$$

The maximum root depth is obtainable from direct measurements or from literature.

Rooting Width

For the lateral extent of the rooting systems over time, the following equation was used:

$$\text{Root width}(t) = [\text{Root width} / \text{Root depth}] \text{ ratio} * \text{root depth}(t) \quad (7)$$

The [Root width/Root depth] ratio is dependent on the crop and the soil type and can be experimentally determined or obtained from literature.

2.3. Relative and Actual Crop Yield

The Relative Crop Yield (RY) is estimated as the sum of the actual water uptake over the season divided by the sum of the maximum water uptake, i.e. the water uptake under no water and salinity stress, as:

$$RY = \frac{\sum S(x, z, t)}{\sum S_{\max}(x, z, t)} \quad (8)$$

where x and z are the horizontal and vertical coordinates, respectively, of each grid cell that contain roots.

The Actual Yield (AY) based on RY is calculated as:

$$AY = RY * Y_{\max} \quad (9)$$

where Y_{\max} is the maximum yield recorded in a given region under stress-free optimum conditions.

Actual yield based on crop growth and biomass production

The AY can also be obtained by calculating the daily biomass production and the harvest index (Eckersten and Jansson, 1991).

1- Increase in Biomass Δq , = Net Assimilation "NA"

"NA" = Assimilation "A" – Respiration losses "R"

2- Assimilation rate "A" = $E * I * f(\text{Temp}) * f(T) * f(\text{Leaf-N})$ (10)

E is the photosynthesis efficiency (g dry matter MJ⁻¹) ≈ 2.0

I is the radiation input = $R_s (1 - e^{-k * LAI})$

R_s is global radiation (MJ m⁻² day⁻¹), k is the extinction coefficient (≈ 0.6) and LAI is the Leaf Area Index (m² m⁻²). R_s is an input and daily LAI is simulated.

In SALTMED model the Assimilation rate "A" per unit area = $E * I * [\text{stress factors related to temperature, transpiration and Leaf Nitrogen content}]$.

2.4. Water and Solute Flow

The soil water flow was simulated using Richard's equation; based on two physical principles: Darcy's law and mass continuity. Darcy's law states:

$$q = -K(h) \frac{\delta H}{\delta Z} \quad (11)$$

q is the water flux, $K(h)$ is the hydraulic conductivity as a function of soil water pressure head, Z is the vertical coordinate directed downwards and H is the hydraulic head which is the sum of the gravity head, Z, and the pressure head, ψ , as:

$$H = \psi + Z \quad (12)$$

The vertical flow of water in the root zone can be described by a Richard's type equation as:

$$\frac{\partial \theta}{\partial t} = -\frac{\partial}{\partial z} \left[K(\theta) \frac{\partial(\psi + z)}{\partial z} \right] - S_w \quad (13)$$

θ is volumetric soil moisture; t is the time; z is the depth; $K(\theta)$ is the hydraulic conductivity (a function of soil moisture); ψ is the matrix suction head; and S_w represents extraction by plant roots.

Although the velocity and direction of solute movement in soils depends on the path of water movement, it is also affected by diffusion and hydrodynamic dispersion. If the latter effects are considered negligible, solute flow by convection can be described as (Hillel, 1977):

$$J_c = qc = \bar{v}\theta c \quad (14)$$

q is the water flux density of the water; J_c is the solute flux density; c the concentration of solute in the flowing water and \bar{v} is the average velocity of the flow.

The solute diffusion rate in bulk water (J_d) is related to the concentration gradient (Fick's law):

$$J_d = D_o(\partial c / \partial x) \quad (15)$$

where D_o is the diffusion coefficient. The diffusion coefficient (D_s) in soil is reduced as the liquid phase only occupies a fraction of soil volume and the path has a tortuous nature. D_s can therefore be expressed as follows:

$$D_s = D_o\theta\xi \quad (16)$$

$$\xi = \theta^{7/3} / \theta_s^2 \quad (17)$$

ξ is the tortuosity, an empirical factor less than unity expected to decrease with decreasing θ (Šimůnek and Suarez, 1994). As the convection flux also causes hydrodynamic dispersion, a sharp boundary between two miscible solutions becomes increasingly diffuse at the mean position of the front. In this case, there is a linear relation between the diffusion coefficient and the average flow velocity \bar{v} (Bresler, 1975):

$$D_h = \alpha\bar{v} \quad (18)$$

α is an empirical coefficient.

The overall solute flux can be obtained by combining the convection, diffusion and dispersion as:

$$J = -(D_h + D_s)(\partial c / \partial x) + \bar{v}\theta c \quad (19)$$

Taking the continuity equation into consideration, one-dimensional transient movement of a non-interacting solute in soil can be expressed as:

$$\frac{\partial(\theta c)}{\partial t} = \frac{\partial}{\partial x} \left(D_a \frac{\partial c}{\partial x} \right) - \frac{\partial(qc)}{\partial x} - S_s \quad (20)$$

c is the solute concentration in the soil solution, q is the convective solute flux, D_a is a combined diffusion and dispersion coefficient and S_s is a sink term represents solute root adsorption/uptake.

The two-dimensional flow of water in the soil can be described according to Bresler (1975) as:

$$\frac{\partial \theta}{\partial t} = \frac{\partial}{\partial x} \left[K(\theta) \frac{\partial \psi}{\partial x} \right] + \frac{\partial}{\partial z} \left[K(\theta) \frac{\partial (\psi + z)}{\partial z} \right] \quad (21)$$

where x is the horizontal co-ordinate; z is the vertical-ordinate (considered to be positive downward); $K(\theta)$ is the hydraulic conductivity of the soil.

When the principal axes of dispersion are oriented parallel and perpendicular to the mean direction of flow, the hydrodynamic dispersion coefficient D_{ij} can be calculated as:

$$D_{ij} = \lambda_T |V| \delta_{ij} + (\lambda_L - \lambda_T) V_i V_j / |V| + D_s(\theta) \quad (22)$$

λ_L is the longitudinal dispersivity of the soil; λ_T is the transversal dispersivity; δ_{ij} is Kronecker delta (i.e., $\delta_{ij}=1$ if $i=j$ and $\delta_{ij}=0$ if $i \neq j$); V_i and V_j are the i^{th} and j^{th} components of the average interstitial flow velocity V , respectively. $V = (V_x^2 + V_z^2)^{1/2}$ and $D_s(\theta)$ is the soil diffusion coefficient. For two dimensional flow, substituting D_{ij} , the solute flow equation becomes:

$$\frac{\partial (C\theta)}{\partial t} = \frac{\partial}{\partial x} \left(D_{xx} \frac{\partial C}{\partial x} + D_{xz} \frac{\partial C}{\partial z} - q_x C \right) + \frac{\partial}{\partial z} \left(D_{zz} \frac{\partial C}{\partial z} + D_{zx} \frac{\partial C}{\partial x} - q_z C \right) \quad (23)$$

In the SALTMED Model, water and solute flow under rainfed conditions and under basin, centre pivot and sprinkler irrigation are simulated by one-dimensional flow equations (Eqs. 13 & 20); under furrow irrigation or irrigation from a trickle line source, two-dimensional flow equations are used (Eqs. 21 & 23); while for drip irrigation, where the drippers are spaced far enough apart so that overlap of the wetting fronts of the adjacent drippers does not take place, “cylindrical flow” equations obtained by replacing x by the radius “ r ” and rearranging Eqs 21 and 23 as described by Bresler (1975) and Fletcher Armstrong and Wilson (1983) are used. In the SALTMED model the water and solute flow equations are solved numerically using a finite difference explicit scheme (Ragab *et al.*, 1984).

Soil Hydraulic Parameters

The “soil water content – water potential” and the “soil water potential – hydraulic conductivity” relationships that are required to solve the water and solute transport equations were taken from van Genuchten (1980).

$$\theta(h) = \theta_r + [(\theta_s - \theta_r) / (1 + |\alpha h|^n)^m] \quad (24)$$

$$K(h) = K_s K_r(h) = K_s S_e^{1/2} [1 - (1 - S_e^{1/m})^m]^2 \quad (25)$$

Where θ_r and θ_s are the residual and the saturated moisture contents, respectively; K_s and K_r are saturated and relative hydraulic conductivity respectively, α and n are shape parameters, $m = 1 - 1/n$ and S_e is effective saturation or normalized volumetric soil water content. α , n and λ are empirical parameters.

Equations 24 & 25 were re-arranged to obtain and the soil water potential and hydraulic conductivity as:

$$S_e = (\theta - \theta_r) / (\theta_s - \theta_r) \quad (26)$$

$$h(S_e) = [(S_e^{-1/m} - 1)^{1/n}] / \alpha \quad (27)$$

$$K(S_e) = K_s S_e^\lambda [1 - (1 - S_e^{1/m})^m]^2 \quad (28)$$

SALTMED Model data base has values of θ_r , θ_s , λ , K_s , water content at field capacity and wilting point, bubbling pressure and n and m (as $n = \lambda + 1$ and $m = \lambda / n$) for several soil types (for users in absence of measurements). The model could also use measured tabulated pair values of both “soil moisture-soil water potential” and “soil moisture - hydraulic conductivity”.

Drainage

SALTMED offers free drainage at the bottom of the root zone, open or tile subsurface drainage systems, and shallow groundwater with no drainage system. The drainage flow equation (Wesseling, 1973), is based on Hooghoudt's drainage equation (Hooghoudt, 1940):

$$qL = (8Hm / L)(K_b \times D_e + K_a \times H_a) \quad (29)$$

q is the steady recharge of water to the water table equal to the drain discharge ($m \text{ day}^{-1}$ or $m \text{ hr}^{-1}$), L is the drain spacing (m), Hm is the height of the water table midway between drains (m), K_b is the hydraulic conductivity of the soil below drain ($m \text{ day}^{-1}$ or $m \text{ h}^{-1}$), K_a is the hydraulic conductivity of the soil above drain ($m \text{ day}^{-1}$ or $m \text{ h}^{-1}$), D_e is Hooghoudt's equivalent depth to the impermeable layer below drain and $H_a = Hm/2$ is the average height of the water table above drain (Figure 1).

Insert figure 1 here

The equivalent depth D_e depends on the depth D of the impermeable layer below the drains as follows:

$$\text{If } D < R: \quad D_e = D \quad (30)$$

$$\text{If } R < D < L/4: \quad De = D \times L / \{(L-D)^2 + 8D \times L \times \ln(D/R)\} \quad (31)$$

$$\text{If } D > L/4: \quad De = L/8 \ln(L/R) \quad (32)$$

R is the drain radius (m). For $L/8 < D < L/2$, Equations 31 and 32 give similar results. Equation 30 is the results of an analysis of Hooghoudt's theory (Wesseling, 1973). Equations 30 and 32 were given by Hooghoudt (1940).

In case of open drains instead of buried pipes, the above equations can be applied using equivalent radius calculated as $R=W/\pi$, where W is the wetted perimeter of the ditch. Further, the equations can be used for drainage with a falling water table (Oosterbaan 1993; Oosterbaan *et al.*, 1989) if the coefficient 8 is changed into 6.4. $W=B+2h$ for rectangular, $W = b + 2h\sqrt{1+z^2}$ for trapezoidal and $W = 2h\sqrt{1+z^2}$ for V shaped ditch. B is bottom breadth, h is height of water and Z is the horizontal distance at which the water height drops by a single unit (side slope), $Z= 0.25$ for rock, 0.5 for hard compact pan, 1.25 for gravel, 1.5 for loam, 2 for loose sandy loam, 2.5 for wet sand, 3 for light sand and wet clay (see details at <http://www.ca.uky.edu/wkrec/openchannelflow.pdf>).

2.5. Calculating Soil Temperature from Air Temperature

The temperature of the top soil (ploughing layer) strongly affects the microbiological activity in this layer and thus the decomposition of organic matter. Based on the work of Zheng *et al.* (1993) and Kang *et al.* (2000), SALTMED considers that the temperature of the top soil is strongly affected by the temperature of the air. The relation is described as:

For $A_j > T_{j-1}(z)$:

$$T_j(z) = T_{j-1}(z) + [A_j - T_{j-1}(z)] * \text{Exp} [-z ((\pi / (k_s * p))^{0.5})] * \text{Exp} [-k(LAI_j + \text{litter}_j)] \quad (33)$$

For $A_j \leq T_{j-1}(z)$:

$$T_j(z) = T_{j-1}(z) + [A_j - T_{j-1}(z)] * \text{Exp} [-z ((\pi / (k_s * p))^{0.5})] * \text{Exp} [-k(\text{litter}_j)] \quad (34)$$

Where A_j is average air temperature at day “j”, in °C, and is calculated from T_{min} and T_{max} , $T_{j-1}(z)$ is the soil temperature at day “j-1” previous day at depth “z” below soil surface, in °C and $T_j(z)$ is the soil temperature at day “j” and depth “z” below soil surface, in °C. $\text{Exp} [-z ((\pi / (k_s * p))^{0.5})]$ is a damping ratio, k_s is the thermal diffusivity as a function of soil water, air and mineral content, $m^2 s^{-1}$, $k_s = [\text{thermal conductivity}/(\text{bulk density} * \text{specific heat capacity})]$, P is the period of either diurnal or annual temperature variation, z is in meters,

LAI is calculated daily by the model, litter fraction is given as user input. The thermal properties of different materials and soils in SALTMED database are taken from Marshall *et al.* (1996).

2.6. Soil Nitrogen Dynamics and Nitrogen Uptake

The nitrogen dynamics considered in the SALTMED are based on the SOIL N Model (Johnsson *et al.*, 1987). Figure 2 shows the processes implemented in SALTMED: mineralization, immobilization, nitrification, denitrification, leaching and plant nitrogen uptake.

It was assumed that nitrogen could enter the system through dry and wet deposition, incorporation of crop residues, application of manure and chemical fertiliser and applied with the irrigation water (fertigation).

Mineralisation of humus, $N_h(z)$, is calculated as a first-order rate process:

$$N_{h \rightarrow NH_4^+}(z) = k_h e_t(z) e_m(z) N_h(z) \quad (35)$$

where k_h is the specific mineralization constant and $e_t(z)$ and $e_m(z)$ are response functions for soil temperature and moisture, respectively.

Insert figure 2 here.

$N_{h \rightarrow NH_4^+}$ is in $g\ N\ m^{-2}\ day^{-1}$, k_h is in day^{-1} , e_t and e_m are dimensionless, $N_h(z)$ is in $g\ N\ m^{-2}$.

Decomposition of soil litter carbon, $C_l(z)$, is a function of a specific rate constant (k_l), temperature and moisture:

$$C_{l(d)}(z) = k_l e_t(z) e_m(z) C_l(z) \quad (36)$$

$C_{l(d)}(z)$ is expressed in $g\ carbon\ m^{-2}\ day^{-1}$; k_l in day^{-1} , e_t and e_m are dimensionless and $C_l(z)$ is in $g\ carbon\ m^{-2}$. The relative amounts of decomposition products formed are governed by a synthesis efficiency constant (f_e) and a humification factor (f_h):

$$C_{l \rightarrow CO_2}(z) = (1 - f_e) C_{l(d)}(z) \quad (37)$$

$$C_{l \rightarrow h}(z) = f_e f_h C_{l(d)}(z) \quad (38)$$

and

$$C_{l \rightarrow l}(z) = f_e (1 - f_h) C_{l(d)}(z) \quad (39)$$

$C_{l \rightarrow CO_2}$, $C_{l \rightarrow h}$ and $C_{l \rightarrow l}$ are expressed in $g\ carbon\ m^{-2}\ day^{-1}$, $C_{l(d)}$ is in $g\ carbon\ m^{-2}$, f_e and f_h are dimensionless.

The net mineralization, or immobilisation, of nitrogen N in litter ($N_l(z)$) is determined from Eqs. (36), (38) and (39):

$$N_{l \rightarrow NH_4}(z) = \left[\frac{N_l(z)}{C_l(z)} - \frac{f_e}{r_o} \right] C_{l(d)}(z) \quad (40)$$

Where $N_{l \rightarrow NH_4}$ is in $g\ N\ m^{-2}\ day^{-1}$; N_l is $g\ N\ m^{-2}$; C_l is $g\ carbon\ m^{-2}$; f_e and r_o , the C-N ratio of microorganisms and of humified products, respectively (dimensionless).

The transfer rate of ammonium to nitrate depends on the potential rate (k_n), which is reduced as the nitrate-ammonium ratio (η_q) is approached:

$$N_{NH_4 \rightarrow NO_3}(z) = k_n e_t(z) e_m(z) \left[N_{NH_4}(z) - \frac{N_{NO_3}(z)}{\eta_q} \right] \quad (41)$$

$N_{NH_4 \rightarrow NO_3}$ is expressed in $g\ N\ m^{-2}\ day^{-1}$, N_{NH_4} and N_{NO_3} are in $g\ N\ m^{-2}$, k_n is in day^{-1} , and η_q , e_t and e_m are dimensionless.

$$e_t(z) = Q_{10}^{\left[\frac{T(z) - t_o}{10} \right]} \quad (42)$$

where $T(z)$ is the soil temperature of the layer, t_o is the base temperature at which $e_t(z)$ equals 1 and Q_{10} is the factor change in rate with a 10-degree change in temperature.

$$e_m(z) = e_s + (1 - e_s) \left[\frac{\theta_s(z) - \theta(z)}{\theta_s(z) - \theta_{ho}(z)} \right]^m \quad \theta_s(z) \geq \theta(z) > \theta_{ho}(z) \quad (43a)$$

$$e_m(z) = 1 \quad \theta_{ho}(z) \geq \theta(z) \geq \theta_{lo}(z) \quad (43b)$$

$$e_m(z) = \left[\frac{\theta(z) - \theta_w(z)}{\theta_{lo}(z) - \theta_w(z)} \right]^m \quad (43c)$$

$$\theta_{lo}(z) > \theta(z) \geq \theta_w(z) \quad (43d)$$

where $\theta(z)$ is the saturated water content, $\theta_{ho}(z)$ and $\theta_{lo}(z)$ are the high and low water contents, respectively, for which the soil moisture factor is optimal and $\theta_w(z)$ is the minimum water content for process activity. The coefficient e_s defines the relative effect of moisture when the soil is completely

saturated and m is an empirical constant. The two thresholds, defining the optimal range are calculated as:

$$\theta_{lo}(z) = \theta_w(z) + \Delta\theta_1 \quad (44a)$$

$$\theta_{ho}(z) = \theta_s(z) - \Delta\theta_2 \quad (44b)$$

where $\Delta\theta_1$ and $\Delta\theta_2$ are the volumetric range of water content where the response increases and decreases, respectively.

The water content is in $m^3 m^{-3}$, soil temperature is in $^\circ C$ and e_t and e_m are dimensionless.

The cumulative potential N demand during the growing season is described by a logistic uptake curve as:

$$\int u(t) dt = \frac{u_a}{1 + \frac{u_a - u_b}{u_b} e^{-u_c t}} \quad (45)$$

where u_a is the potential annual N uptake, u_b and u_c are shape parameters and t is days after the start of the growing season, u_a is expressed in $g N m^{-2} season^{-1}$.

Daily uptake of nitrate is calculated from the relative root fraction in the layer ($f(z)$), the proportion of total mineral N as nitrate and the derivative of the growth curve (u). u is calculated by Eq. 45 on daily basis, expressed as $gram N m^{-2} day^{-1}$, $N_{NO_3}(z)$ and $N_{NH_4}(z)$ are in $g N m^{-2}$.

$$N_{NO_3 \rightarrow p}(z) - MIN \text{ of } f_r(z) \frac{N_{NO_3}(z)}{N_{NO_3}(z) + N_{NH_4}(z)} u \quad (46a)$$

and

$$f_{ma} N_{NO_3}(z) \quad (46b)$$

The denitrification rate is described by a power function that increases from a threshold ($\theta_d(z)$) and is maximum at saturation [$\theta_s(z)$], where d is an empirical constant.

$$e_{md}(z) = \left[\frac{\theta(z) - \theta_d(z)}{\theta_s(z) - \theta_d(z)} \right]^d \quad (47)$$

The denitrification rate of each layer depends on a potential denitrification rate ($k_d(z)$), the soil water/aeration statue [$e_{md}(z)$] and the temperature factor [$e_t(z)$] similarly used for the other biologically-controlled processes.

$$N_{NO_3 \rightarrow}(z) = k_d(z)e_{md}(z)e_t(z) \left[\frac{[N_{NO_3}(z)]}{[N_{NO_3}(z)] + C_s} \right] \quad (48)$$

$N_{NO_3 \rightarrow}(z)$ and $k_d(z)$ are expressed in $g\ N\ m^{-2}\ d^{-1}$, $N_{NO_3}(z)$ is in $g\ N\ m^{-2}$, C_s is in $mg\ l^{-1}$, e_t and e_{md} are dimensionless. The rate constants and parameter values obtained under field conditions by Wu *et al.* (1989) can be used in SALTMED in absence of measured values.

3. Model Application

SALTMED's database contains a large number of soils parameters, crop parameters and nitrogen parameters, which could be used in absence of measurements.

3.1. Examples of model runs

The model runs with up to 20 fields or treatments or rotations. This facility allows simultaneous runs of different actual systems of soil, crop, irrigation, N-fertilizers and allows “what if” scenarios as model application in forecasting /prediction mode. Figure 3 shows some examples of graphic output during the model run.

[Insert figure 3 here](#)

3.2. Modelling and field studies

The following is a summary of results obtained using SALTMED model within the SWUP-MED project, full papers on these examples are expected to follow this paper in the Journal of Irrigation and Drainage.

Use of saline water for irrigation

SALTMED model was applied on field experiment using saline water for irrigation of quinoa in Italy, Denmark and Turkey; amaranth in Italy; and legumes in Syria. The model quantified the salinity tolerance level and the threshold values of each crop. Quinoa and amaranth grown in Italy were most tolerant at salinity level of $22\ dS\ m^{-1}$ with limited yield reduction, even when using 25% of the crop water requirement. In the Denmark study, using water salinity up to $40\ dS\ m^{-1}$, quinoa yield was only reduced by 17% when compared with fresh water irrigation. The study in Turkey showed there was hardly any yield reduction when irrigating quinoa with water of salinity up to $30\ dS\ m^{-1}$, the reduction only becoming apparent when the water added was dropped to 33% of the full irrigation. The results showed the possibility of significant water saving with acceptable reduction level in yield. Legumes grown in Syria showed relatively less salinity tolerance. Fresh water and up water with salinity up to $5\ dS\ m^{-1}$ was used to irrigate faba bean, lentil, and chickpea. The threshold value of 50% yield reduction

in lentil, chickpea, and faba bean occurred at salinity levels of 3.6 dS m⁻¹, 4.4 dS m⁻¹ and 5.4 dS m⁻¹, respectively.

Use of deficit irrigation

In Agadir, Morocco, quinoa and sweet corn (C3 crops) and chickpea (C4 crop), were subjected to different water stresses at different growth stages. Results showed that the yield was not affected when the water stress took place during the vegetative growth stage. The study also showed the ability of the SALTMED model to account for the differences in photosynthesis efficiency between C3 and C4 crops. A deficit irrigation experiment in Marrakech, Morocco, showed that there was only 15% yield reduction when quinoa received 50% of its total water requirement. A study in Agadir, Morocco on five accessions of quinoa, using deficit irrigation, indicated some variations among the accessions with a reduction in yield varying from 9% to 49% when applying 50% of the crop water requirement. A comparative study conducted in Portugal on five varieties chickpea grown during a wet year and a dry year with supplementary irrigation showed that the 'wet year' yields were lower than the 'dry year' yields, although the total amounts of water the crop received from rain + irrigation were comparable. This highlights the importance of irrigation timing; the unpredictable rainfall might not be used efficiently by the plant if it falls in large amounts or at the wrong time.

Use of treated wastewater, organic manure and deficit irrigation

The model was used to simulate sweet corn growth and yield in Morocco when using waste water, deficit irrigation strategy at different growth stages and organic matter amendment. The results indicated that flowering and grain filling stages were the most sensitive to deficit irrigation, while the vegetative growth stage was the most tolerant. The yield response to water stress levels equal to 75%, 50%, 25% and 0% of the full irrigation amount, applied during vegetative growth stage showed that applying 25% of full irrigation requirement had not significantly affected sweet corn yield. This means that 75% water saving during the vegetative growth, representing 20% saving of total seasonal water requirement can be achieved without significant reduction in the yield. The results also indicated that organic amendment of 10 t ha⁻¹ and 5 t ha⁻¹ increased sweet corn yield by 15 and 1%, respectively, under full irrigation conditions; and by 10 and 4%, respectively, under deficit irrigation applying 50% of the full irrigation requirement.

Crop rotation

Crop rotations of quinoa, sweet corn and three legume crops were investigated in Morocco. Quinoa and sweet corn yields were higher when they were sown after fallow, while chickpea as previous crop to quinoa had a better impact on quinoa yield than faba bean.

Possible impact of future climate change scenarios

Two studies were carried out using SALTMED's facility to allow crops to grow according to the number of heat units or degree days, which is of particular interest for climate change impact studies.

In Morocco, the simulations were carried out using sweet corn. For the crop growth model, the degree days option was adopted. The SALTMED model was run with 6 periods corresponding to 2015, 2020, 2030, 2050, 2075 and 2090. The results showed an earlier harvest date as well as a shorter growing season as time progresses from 2015 to 2090 in response to increasing temperature due to climate change. The length of the growing period might be reduced by about 20 days. The simulation results also showed that from 2020 to 2075 there will be a decrease in terms of total produced dry matter and yield. The evapotranspiration, as well as potential crop transpiration, might increase in response to climate change.

In Italy, the productivity of amaranth A12 under different climate scenarios, based on changes in temperature, was simulated using crop calibrated data of amaranth. Two climate scenarios, 2050 and 2095, based on the outputs of six GCMs were considered. The simulations were performed using temperature data generated from GCMs and the SALTMED model option of variable sowing and harvest date. The SALTMED model indicated that the length of the amaranth growing season will decrease from 114 days under actual (2009-2010) climatic conditions to 98 days for the high emission scenarios in 2095. SALTMED also indicated that it is possible to expect a change in amaranth sowing date from the day of the year (DOY) 100 under actual conditions to the DOY 86 by 2095. The use of GCM and SALTMED could be a useful decision system for sustainable agronomic management.

All the study cases undertaken within the SWUP-MED project proved the SALTMED model can be a very useful management tool for academics, field managers and IT-educated farmers.

Acknowledgement

The SALTMED model has been developed with support of the EU funded projects, SALTMED, SAFIR, SWUP-MED, and Water4Crops. The results reported here are largely based on the efforts of the SWUP-MED project colleagues whose full papers will follow this paper.

References

- Allen GR, Pereira LS, Raes D, Smith M. 1998. Crop evapotranspiration. *Irrigation and Drainage Paper No. 56*. FAO, Rome, Italy.
- Bresler E. 1975. Two-dimensional transport of solute during non-steady infiltration for a trickle source. *Soil Science Society of America Proceedings* **39**: 604-613.
- Cardon EG, Letey J. 1992. Plant water uptake terms evaluated for soil water and

solute movement models. *Soil Science Society of America Journal* **56**: 1876-1880.

Choukr-Allah R. 2012. Perspectives of Wastewater Reuse in the Mediterranean Region. In *Integrated Water Resources Management in the Mediterranean Region* (Eds. Choukr-Allah R, Ragab R, Rodriguez-Clemente R), pp. 125-137. Springer, The Netherlands. doi:10.1007/978-94-007-4756-2_8

ECKERSTEN, H. & JANSSON, P-E. (1991). Modelling water flow, nitrogen uptake and production for wheat. *Fertilizer Research* **27**, 313-329.

Fletcher Armstrong C, Wilson TV. 1983. Computer model for moisture distribution in stratified soils under trickle source. *Transactions of American Society of Agricultural Engineers* **26**: 1704-1709.

Golabi M, Naseri AA, Kashkuli HA. 2009. Evaluation of SALTMED model performance in irrigation and drainage of sugarcane farms in Khuzestan province of Iran. *J Food Agric Environ* **7**: 874-880.

Hamdy A, Ragab R, Scarascia ME. 2003. Coping with water scarcity: Water saving and increasing water productivity. *Journal of Irrigation and Drainage* **52**: 3-20.

Hillel D. 1977. *Computer simulation of soil-water dynamics; a compendium of recent work*. (Ed. Hillel D) 214p. IDRC, Ottawa, Canada.

Hirich A, Choukr-Allah R, Ragab R, Jacobsen S-E, Youssfi LE, Omari HE. 2012. The SALTMED model calibration and validation using field data from Morocco. *Journal of Materials and Environmental Sciences* **3(2)**: 342-359.

Hirich A, Ragab R, Choukr-Allah R, Rami A. 2013. The effect of deficit irrigation with treated waste water on sweet corn: Experimental and modelling study using SALTMED model. *Irrigation science*. In press: DOI: 10.1007/s00271-013-0422-0

Hooghoudt SB. 1940. General consideration of the problem of field drainage by parallel drains, ditches, watercourses, and channels. Publ. No.7 in the series *Contribution to the knowledge of some physical parameters of the soil* (titles translated from Dutch). Bodemkundig Instituut, Groningen, The Netherlands.

Huibers FP, Raschid-Sally L, Ragab R (Editors). 2005. Editorial, Wastewater Irrigation, *Journal of Irrigation and Drainage* **54**: 1-2.

Jarvis PG. 1976. The interpretation of the variations in leaf water potential and stomatal conductance found in canopies in the field. Philosophical. *Transactions of the Royal Society*. B273, 593-610.

Johnsson H, Bergstrom L, Jansson P-E. 1987. Simulated nitrogen dynamics and losses in a layered agricultural soil. *Agriculture, Ecosystems and Environment* **18**: 333-356.

Kang S, Kim S, Oh S, Lee D. 2000. Predicting spatial and temporal patterns of soil temperature based on topography, surface cover and air temperature. *Forest Ecology and Management* **136**:173-184.

Körner C. 1994. Leaf diffusive conductance in the major vegetative types of the globe. In *Ecophysiology of Photosynthesis* (Eds E. D. Schulze & M. M. CALWELL) *Ecological Studies*, Vol.100. Springer Verlag, Berlin, pp 463-490.

Körner C. 1995. Impact of atmospheric changes on alpine vegetation: the ecophysiological perspective. In *Potential ecological impacts of climate change in the Alps and Fennoscandian mountains* (Eds. Guisan A, Holten JI, Spichiger R, Tessier L), *Ed. Conservatoire et Jardin Botaniques de Genève*, pp. 113-120.

- Malash N, Flowers TJ, Ragab R. 2005. Effect of irrigation systems and water management practices using saline and non-saline water on tomato production. *International Journal of Agricultural Water Management* **78** (1-2): 25-38.
- Malash NM, Flowers TJ, Ragab R. 2008. Effect of irrigation methods, management and salinity of irrigation water on tomato yield, soil moisture and salinity distribution. *Irrigation Science* **26**: 313-323.
- Malash NM, Flowers TJ, Ragab R. 2011. Plant water relations, growth and productivity of tomato irrigated by different methods with saline and non-saline water. *Irrigation and Drainage* **60** (40): 446-453.
- Marshall TJ, Holmes JW, Rose CW (Eds). 1996. Soil Physics (3rd edition), pp. 358-376. Cambridge University Press. Cambridge, UK.
- Monteith JL. 1965. Evaporation and the environment. XIXth Symposia of the Society for Experimental Biology. In *The State and Movement of Water in Living Organisms*, pp. 205–234. University Press, Swansea, Cambridge.
- Montenegro S, Montenegro A, Ragab R. 2010. Improving agricultural water management in the semi-arid region of Brazil: experimental and modelling study. *Irri Sci* **28**: 301-316.
- Oosterbaan RJ. 1993. Hooghoudt's drainage equation, adjusted for entrance resistance and sloping land. International Institute for Land Reclamation and Improvement (ILRI), P.O. Box 45, 6700 AA Wageningen, The Netherlands, 1993. Updated version of “Interception drainage and drainage of sloping lands” of same author published in: *Bulletin of the Irrigation, Drainage and Flood Control Council, Pakistan*, Vol. 5, No. 1, June 1975. On the web: www.waterlog.info/faqs.htm.
- Oosterbaan RJ, Pissarra A, Van Alphen JG. 1989. Hydraulic head and discharge relations of pipe drainage systems with entrance resistance. *Proceedings 15th European Conference on Agricultural Water Management Vol. III: Installation and Maintenance of Drainage and Irrigation Systems*. Pp. 86-98. ICID, Dubrovnik, Yugoslavia.
- Plauborg F, Andersen MN, Liu F, Ensink J, Ragab R. 2010. Safe and high quality food production using low quality waters and improved irrigation systems and management: SAFIR. *Agricultural Water Management* **98**, 377-384. 10.1016/j.agwat.2010.05.020
- Pulvento C, Riccardi M, Lavini A, D'Andria R, Ragab R. 2013. SALTMED model to simulate yield and dry matter for quinoa crop and soil moisture content under different irrigation strategies in south Italy. *Irrigation and Drainage* **62** (2): 229-238.
- Ragab R. 2002. A holistic generic integrated approach for irrigation, crop and field management: the SALTMED model. *Environmental Modelling and Software* **17**: 345-361.
- Ragab R, Feyen J, Hillel D. 1984. Simulating two-dimensional infiltration into sand from a trickle line source using the matric flux potential concept. *Soil Science* **137**: 120-127.
- Ragab R (Ed). 2005. Advances in integrated management of fresh and saline water for sustainable crop production: Modelling and practical solutions. *International Journal of Agricultural Water Management* (Special Issue), **78** (1-2): 1-164. Elsevier, Amsterdam, The Netherlands.

Ragab R, Malash N, Abdel Gawad G, Arslan A, Ghaibeh A. 2005. A holistic generic integrated approach for irrigation, crop and field management: 2. The SALTMED model validation using field data of five growing seasons from Egypt and Syria. *International Journal of Agricultural Water Management* **78** (1-2); 89-107.

Ragab R. 2010. SALTMED Model as an integrated management tool for water, crop, soil and fertilizers. In *Manejo da salinidade na agricultura: Estudos básicos e aplicados* (Eds H. R. Gheyi, N. S. Dias, C.F. de Lacerda) pp.320-336. Instituto Nacional de Ciência e Tecnologia em Salinidade, Fortaleza, Brazil.

Razzaghi F, Plauborg F, Ahmadi SH, Jacobsen S-E, Andersen MN, Ragab R. 2011. Simulation of quinoa (*Chenopodium quinoa* willd.) response to soil salinity using the SALTMED model, ICID 21st International Congress on Irrigation and Drainage, 15-23 October 2011. *International Commission on Irrigation and Drainage*, Tehran, Iran, pp 25-32.

Rhoades JD, Kandiah A, Mashali AM. 1992. The use of saline waters for crop production. *FAO, Irrigation and Drainage Paper No 48*. Rome, Italy.

Šimůnek J, Suarez DL. 1994. Two-dimensional transport model for variably saturated porous media with major chemistry. *Water Resources Research* **30**: 1115-1133.

Silva L, Ragab R, Duarte I, Lourenço E, Simões N, Chaves M. 2012. Calibration and validation of SALTMED model under dry and wet year conditions using chickpea field data from Southern Portugal. *Irrigation Sci* **30**:1-9.

Tardieu F, Zhang J, Gowing DJG. 1993. Stomatal control by both [ABA] in the xylem sap and leaf water status: a test of a model for droughted or ABA-fed field-grown maize. *Plant, Cell and Environment* **16**: 413-420.

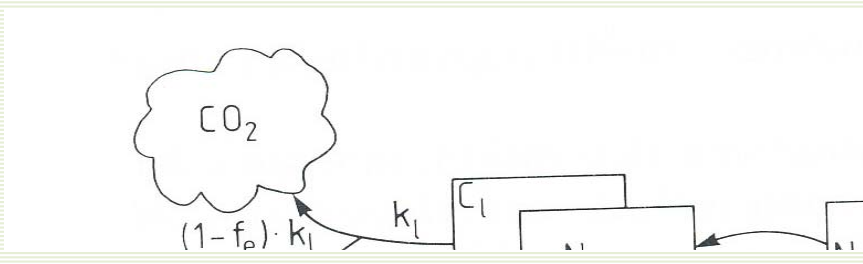
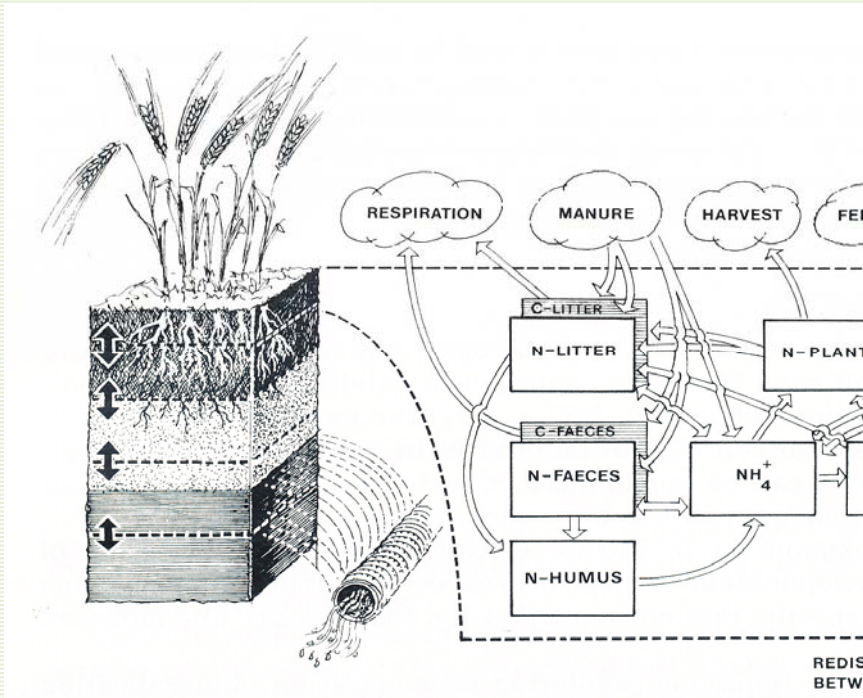
Van Genuchten MTh. 1980. A closed - form equation for predicting the hydraulic conductivity of unsaturated soils. *Soil Science Society of America Journal* **44**: 892-898.

Wesseling J. 1973. Subsurface flow into drains. *Drainage Principles and Applications Vol. II: Theories of Field Drainage and Watershed Runoff*. Pp. 2-56. Publ.16. ILRI, Wageningen, The Netherlands.


Wu L, McGechan MB, Lewis DR, Hooda PS, Vinten AJA. 1998. Parameter selection and testing the soil nitrogen dynamics model SOILN. *Soil Use and Management* **14**: 170-181.

Zheng D, Hunt, Jr., Running, SW. 1993. A daily soil temperature model based on air temperature and precipitation for continental applications. *Climate Research* **2**: 183-191.

Figure 2: Soil nitrogen cycle and processes according to Johnsson *et al.* (1987)




SALTMED Version 3.03.19



Copyright © 2013 Centre for Ecology and Hydrology,
Wallingford, OX10 8BB, UK. All rights reserved

SALTMED





Licensed Material. This computer program is the property of the Centre for Ecology and Hydrology,
Wallingford. All rights reserved.
It is protected under UK and International copyright laws.

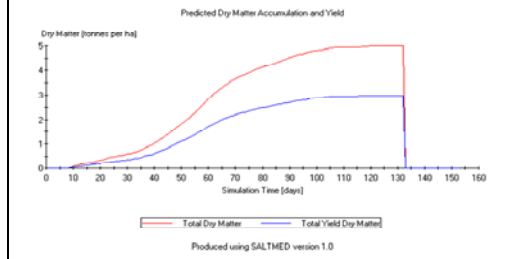
<http://www.ceh.ac.uk>

SALTMED has been developed under three projects:
SALTMED project (1998-2002), EU contract: ERB351PL972469,
then under SAFIR project (2006-2009), EU contract: Food-CT-2005-023168
and currently under SWUP-MED project (2008-2012), EU contract: KBBE-2008- 212337.
These projects are jointly funded by the Natural Environment Research Council, NERC, UK.

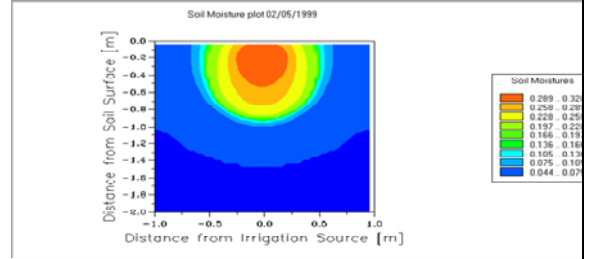
Project Leader: Dr. Ragab Ragab
eMail: rag@ceh.ac.uk

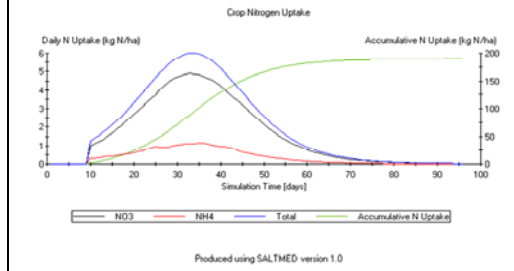
Output example of Dry matter



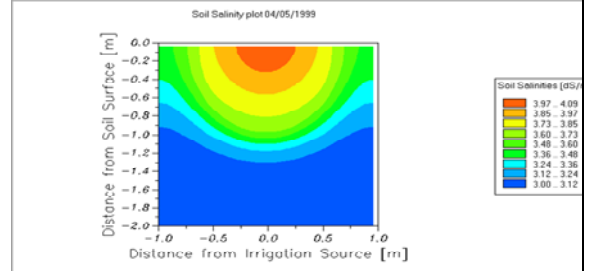
Output example of soil moisture under drip irrigatio



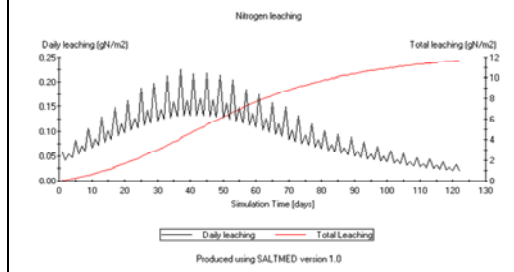
Output example of plant -N uptake



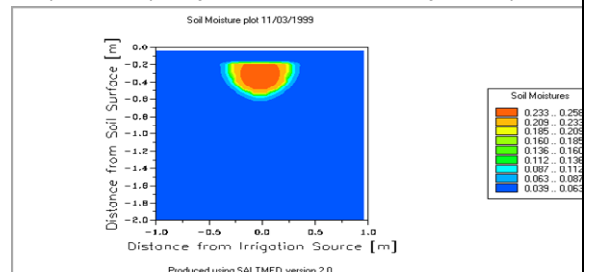
Output example of soil salinity under drip irrigation



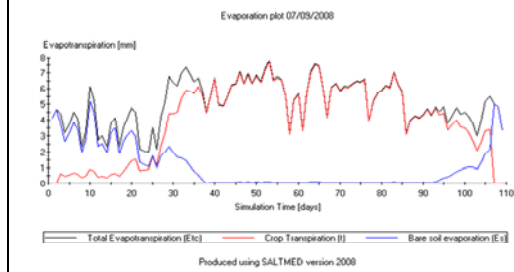
Output example of N- Leaching



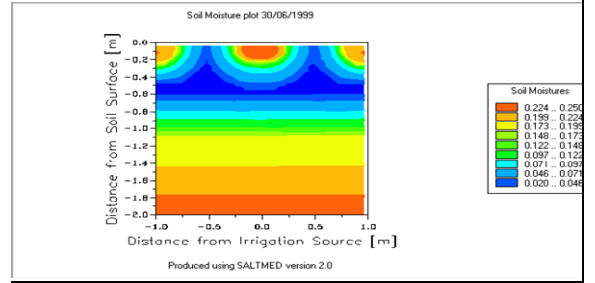
Output example of soil moisture, subsurface drip



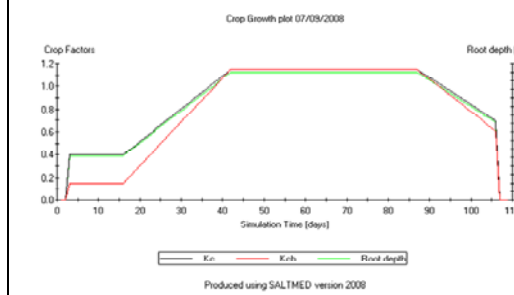
Output example of Evapotranspiration



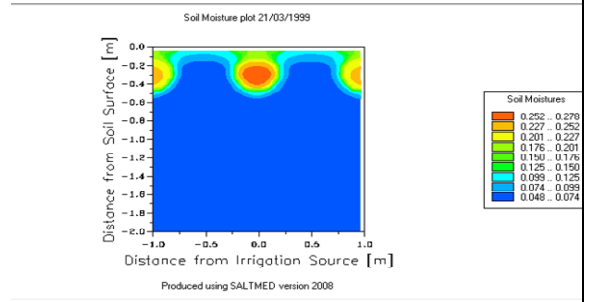
Output example of soil moisture under PRD drip



Output example of crop growth parameters



Output example of soil moisture, PRD subsurface drip



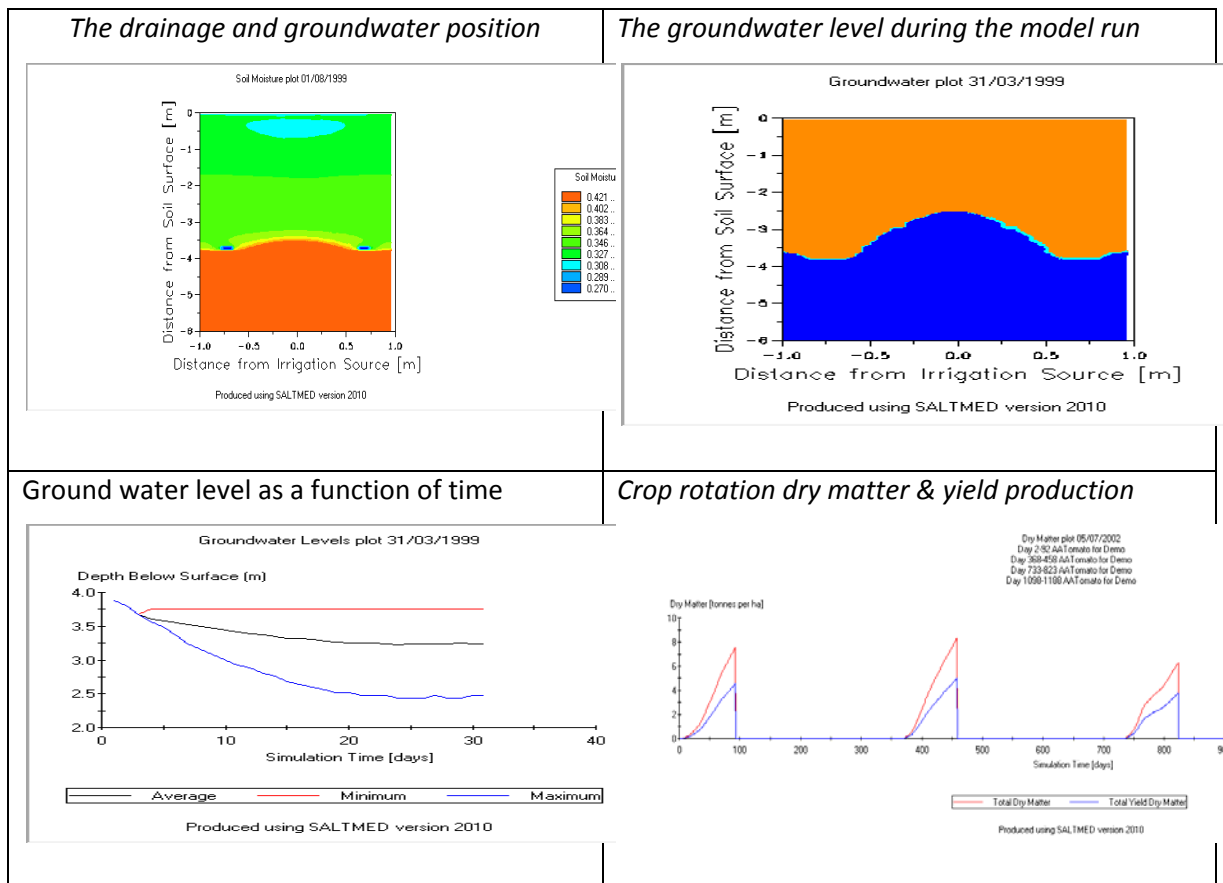


Figure 3. SALTMED output examples